

Numerical Analysis of Moisture Influential Depth in Concrete During Drying-Wetting Cycles*

LI Chunqiu (李春秋), LI Kefei (李克非)**, CHEN Zhaoyuan (陈肇元)

Key Laboratory of Structural Engineering and Vibration of Ministry of Education,
Department of Civil Engineering, Tsinghua University, Beijing 100084, China

Abstract: The influential depth of moisture transport in a concrete surface subject to drying-wetting cycles was analyzed numerically. The moisture transport was described by a diffusion model with different diffusivities for drying and wetting. A finite difference scheme was developed to solve the partial differential equations. The influential depth was then investigated numerically for initially saturated and unsaturated concretes exposed to drying-wetting actions in marine environments using an equilibrium time ratio concept. The equilibrium time ratio was calculated numerically for a saturated condition and the moisture influential depth is shown to be a linear function of the square root of the drying time. However, this equilibrium time ratio does not exist for an unsaturated condition and the moisture influential depth depends on the initial saturation as well as the drying-wetting time ratio. The results indicate that this model gives more realistic predictions of moisture transport of *in situ* structural concrete and its durability.

Key words: concrete; drying-wetting cycles; influential depth; durability

Introduction

The durability of concrete structures is mostly related to moisture transfer, and in particular, the ingress of chloride ions into reinforced concrete members in marine environments^[1]. Multiple moisture transport models have been proposed based on three main mechanisms: absorption, diffusion, and permeation^[2,3]. Drying-wetting cycles are identified as the most unfavorable conditions for aggressive external agent ingress since surface absorption is mobilized to more efficiently transport water soluble agents into concrete. The unified diffusion model^[4-7] cannot give realistic predictions of the moisture transport during drying-wetting cycles because the concrete diffusivity must be

treated separately for drying and wetting processes^[8].

Motivated by the dearth of credible predictions of moisture transport into concrete during drying-wetting cycles, this study used a numerical approach to analyze intrinsic relations among the moisture influential depth, material transport properties, as well as the drying-wetting cycles.

1 Diffusion-Absorption Model of Moisture Transport

1.1 Global transport modeling

A unified diffusion equation is usually used to describe the global moisture transport in concrete^[3],

$$\frac{\partial \theta}{\partial t} = \frac{\partial}{\partial x} \left(D(\theta) \frac{\partial \theta}{\partial x} \right) \quad (1)$$

where θ is the water saturation in the concrete pores, x the coordinate (mm), t the time (s), and D the saturation-dependent moisture diffusivity ($m^2 \cdot s^{-1}$). Note that

Received: 2007-04-25; revised: 2008-01-15

* Supported by the National Natural Science Foundation of China
(No. 50538060)

** To whom correspondence should be addressed.

E-mail: likefei@mail.tsinghua.edu.cn; Tel: 86-10-62797422

Eq. (1) is somewhat simplified and must be used with caution. More sophisticated models are provided by Mainguy and Coussy^[9,10]. For the one-dimensional case, the initial moisture content is described by an initial moisture profile,

$$\theta(x, t=0) = \theta_{\text{ini}}(x) \quad (2)$$

and the Dirichlet boundary condition at the surface for varying moisture conditions is

$$\theta(x=0, t>0) = \theta_s(t) \quad (3)$$

with $\theta_s(t)$ as the prescribed varying water saturation degree at the boundary, $x=0$. To simulate a semi-infinite case, an additional boundary condition is needed,

$$\theta(x=\infty, t>0) = \theta_{\text{ini}}(\infty) \quad (4)$$

1.2 Diffusivity for drying and wetting

As the concrete surface is subject to drying-wetting cycles, the moisture is driven out from the inside of the material by pore water evaporation as well as vapor diffusion during drying, while during the subsequent wetting the moisture transport into the concrete is dominated by surface absorption and possibly vapor diffusion^[11,12]. Thus concrete diffusivities in Eq. (1) during drying and wetting should differ,

$$D(\theta) = \begin{cases} D_d(\theta), & \text{during drying;} \\ D_w(\theta), & \text{behind the wetting front during wetting} \end{cases} \quad (5)$$

The diffusivity during drying is given by the well established relation between the diffusivity and the water saturation^[13],

$$D_d = D_d^s \left(\alpha_0 + \frac{1 - \alpha_0}{1 + \left(\frac{1 - \theta}{1 - \theta_c} \right)^N} \right) \quad (6)$$

where D_d^s is the concrete diffusivity when totally saturated ($\text{m}^2 \cdot \text{s}^{-1}$), and α_0 , θ_c , and N are experimental parameters.

The diffusivity during wetting can only be deduced indirectly since it represents the absorption processes by diffusion. The term “wetting” here refers to the situation when a moisture film with enough thickness accumulates on the concrete surface so that capillary absorption can take place. Hall^[14] deduced the wetting diffusivity from capillary absorption data as

$$D_w(\theta) = D_w^0 \exp(n\theta) \quad (7)$$

with D_w^0 denoting the wetting diffusivity for a totally dry state and n a regression coefficient. Hall^[14]

suggested $n=6-8$ for building materials while Leech et al.^[15] suggested $n=6$ for concrete on the basis of the nuclear magnetic resonance (NMR) imaging analysis of wetting front. In addition, an explicit relation between concrete sorptivity and diffusivity is given by Lockington et al.^[16],

$$\left(\frac{S}{\varphi} \right)^2 = D_w^0 \left[\exp(n) \left(\frac{2}{n} - \frac{1}{n^2} \right) - \left(\frac{1}{n} - \frac{1}{n^2} \right) \right] \quad (8)$$

where S indicates the concrete sorptivity for a totally dry state ($\text{m} \cdot \text{s}^{-1/2}$) and φ is the capillary porosity.

2 Numerical Solution of Moisture Transport

Equations (1)-(7) give a complete model for concrete subject to drying-wetting cycles based on the important assumptions that (1) the drying-wetting processes are isothermal, (2) the external hydraulic pressure and gravity are both neglected compared to capillary absorption for the moisture uptake during wetting, and (3) hysteresis is not taken into account for the moisture transport during the drying-wetting cycles.

With the drying-wetting cycles expressed as the variable moisture boundary condition in Eq. (3), the solution for the time-dependent moisture content distributions was found using a finite difference method. An implicit predictor-corrector scheme^[17] was used to calculate numerical solutions to Eq. (1) with Eq. (2) as the initial condition and Eqs. (3) and (4) as boundary conditions. The scheme ensures 2nd-order accuracy. The central idea of the scheme is, for a given time interval τ , to discretize temporally Eq. (1) into two sub-steps with the first predicted solution for the water saturation,

$$\frac{\theta_j^{k+1/2} - \theta_j^k}{\tau/2} = \frac{1}{h^2} \left[D \left(\frac{\theta_j^k + \theta_{j+1}^k}{2} \right) \left(\theta_{j+1}^{k+1/2} - \theta_j^{k+1/2} \right) - D \left(\frac{\theta_j^k + \theta_{j-1}^k}{2} \right) \left(\theta_j^{k+1/2} - \theta_{j-1}^{k+1/2} \right) \right] \quad (9)$$

and the corrected solution,

$$\frac{\theta_j^{k+1} - \theta_j^k}{\tau} = \frac{1}{h^2} \left[D \left(\frac{\theta_j^{k+1/2} + \theta_{j+1}^{k+1/2}}{2} \right) \left(\frac{\theta_{j+1}^k + \theta_{j+1}^{k+1}}{2} - \frac{\theta_j^k + \theta_j^{k+1}}{2} \right) - D \left(\frac{\theta_j^{k+1/2} + \theta_{j-1}^{k+1/2}}{2} \right) \left(\frac{\theta_j^k + \theta_j^{k+1}}{2} - \frac{\theta_{j-1}^k + \theta_{j-1}^{k+1}}{2} \right) \right] \quad (10)$$

where h is the element length and θ_j^k is the water saturation at node j for $t = k\tau$. The equations were solved with the discretized initial condition of Eq. (2) and the boundary conditions of Eqs. (3) and (4) using a generalized minimal residual method (GMRES) with a preconditioning technique^[18]. The water saturation, θ , was then calculated for all the nodes in space at all times. The element size, h , and time interval, τ , were reduced until the results converged to an expected tolerance.

3 Numerical Analysis of the Influential Depth

3.1 Equilibrium drying-wetting ratio

Natural drying-wetting cycles were idealized as periodic drying-wetting cycles with a drying period, t_d , and a wetting period, t_w . The general variable moisture boundary condition in Eq. (3) was then specified as

$$\theta(x=0, t>0) = \theta_s(t) = \begin{cases} \theta_d, & \text{during drying;} \\ 1.0, & \text{during wetting} \end{cases} \quad (11)$$

Thus, the drying is idealized by imposing a constant water saturation, θ_d , at the concrete surface with the wetting characterized by a constant surface saturation equal to 100%. These boundary conditions were used to investigate the moisture transport influential depth.

First, consider the equilibrium between the moisture loss during drying and the moisture absorbed during the subsequent wetting. For equilibrium, the moisture loss is equal to the moisture absorbed; thus the drying front created at the end of t_d is totally restored during the wetting period, t_w . For a specific drying-wetting cycle scheme, the drying-wetting time ratio at equilibrium is defined as

Table 1 Retained parameters of concrete properties under drying and wetting

| Material | W/C | $D_d^s/10^{-10}(\text{m}^2\cdot\text{s}^{-1})$ | α_0 | θ_c | N | $D_w^0/10^{-10}(\text{m}^2\cdot\text{s}^{-1})$ | n |
|--------------|------|--|------------|------------|------|--|-----|
| Concrete I | 0.40 | 2.00 | 0.025 | 0.792 | 6.00 | 3.22 | 6 |
| Concrete II | 0.50 | 3.15 | 0.025 | 0.792 | 6.00 | 4.24 | 6 |
| Concrete III | 0.60 | 4.23 | 0.025 | 0.792 | 6.00 | 9.45 | 6 |

For Concrete I in Table 1, θ_d is equal to 0.6 and the drying periods, t_d , were 0.5, 1, 5, 10, and 30 days. The corresponding shortest wetting periods, t_w , necessary to restore the moisture loss during drying are found numerically with the results presented in Fig. 1. The results show that an equilibrium time ratio, η_{eq} , does

$$\eta_{eq} = \left. \frac{t_d}{t_w} \right|_{\text{equilibrium}} \quad (12)$$

Analysis of the constitutive Eqs. (1)-(7) and (11) shows that this time ratio, η_{eq} , when it exists, is governed by the concrete diffusivity during drying, the diffusivity during wetting, the initial water saturation profile, and the external drying water saturation,

$$\eta_{eq} = \eta_{eq}(D_d, D_w; \theta_{ini}, \theta_d) \quad (13)$$

where the diffusivities are intrinsic properties of the concrete and the water saturations are external factors.

The equilibrium time ratio can be used to evaluate the moisture influential depth as well as its evolution. If $t_d/t_w \leq \eta_{eq}$, the moisture loss during drying is totally restored during wetting and the influential depth is determined by the drying time t_d . If $t_d/t_w > \eta_{eq}$, the moisture loss is not totally restored by the wetting and the influential depth will progress after each cycle. The equilibrium time ratio can be determined numerically and used to evaluate the moisture influential depth for various drying-wetting cycles for both initially saturated and unsaturated concrete.

3.2 Saturated concrete subject to drying-wetting cycles

For initially saturated concrete, the initial condition in Eq. (2) can be specified as

$$\theta_{ini}(x) = 1.0 \quad (14)$$

The drying properties and softivities of concrete specimens with different water cement ratio (W/C) measured by Wong et al.^[3] are used in the numerical analysis in this section with the corresponding wetting diffusivities, D_w^0 , calculated using Eq. (8). The parameters are summarized in Table 1.

exist and is about 120 for this case. The calculations used a numerical tolerance $\delta=0.01$ to judge whether the moisture was restored in the dried zone by the wetting,

$$\theta(x)|_{t=t_d+t_w} \geq 1.0 - \delta \quad (15)$$

The equilibrium time ratio, η_{eq} , was also calculated for the other two concrete specimens in Table 1 for

four different drying gradients ($1.0 - \theta_d$) of 0.2, 0.4, 0.6, and 0.8. The numerical results in Fig. 2 show that, as indicated in Eq. (13), η_{eq} is mainly influenced by the concrete transport properties and the external drying. The numerical results also show that η_{eq} is less sensitive to the drying gradient than the concrete diffusivity with no direct correlation found between η_{eq} and the drying gradient or between η_{eq} and W/C . This is possibly due to the specific expressions used for the drying and wetting diffusivities.

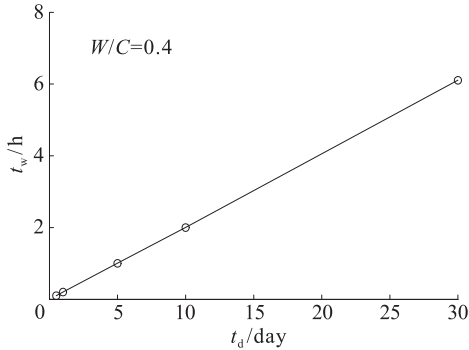


Fig. 1 Equilibrium wetting periods for various drying periods for Concrete I

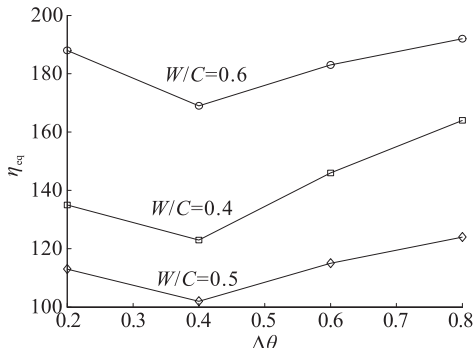


Fig. 2 Equilibrium time ratios for various drying gradient and W/C

The moisture influential depth was then also analyzed. As mentioned before, for a concrete with specified transport properties, the evolution of influential depth is determined by η_{eq} for the drying-wetting cycles, the drying time, t_d , and the wetting time, t_w . The total cycle time t_{d-w} can be expressed as

$$t_{d-w} = t_d + t_w = \left(1 + \frac{1}{\eta}\right) t_d \quad (16)$$

Consider a typical case of sea water splashing where the splashing is considered as a daily event, i.e., $t_{d-w} = 1$ day in Eq. (16). The drying time, t_d , is treated as a variable with values of 0.25, 1, 4, 9, 16, 23, and 23.5 h. The properties of Concrete I in Table 1 were used with

the surface water content taken as 0.6 during drying period. From the time ratio, η_{eq} , in Fig. 1, t_d at equilibrium is 23.8 h. Thus, the wetting time necessary to restore the moisture loss is only about 0.2 h, which means that, for most natural cases, the moisture equilibrium will always be preserved. Accordingly, the drying zone created during drying phase totally disappears by the end of the wetting phase. The moisture influential depth is thus determined by the drying time. The calculated influential depths, ΔX , are illustrated in terms of $t_d^{1/2}$ in Fig. 3. The influential depth is linearly related to the square root of the drying time with the maximum influential depth corresponding to the drying time at the equilibrium ratio, η_{eq} . The maximum depth for these conditions is 11 mm which coincides with the convection zone depth, 6.0–11.0 mm, suggested by the FIB Model Code^[19].

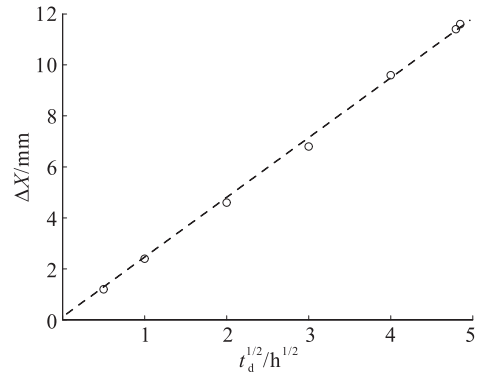


Fig. 3 Moisture influential depth in terms of the square root of the drying time

3.3 Unsaturated concrete subject to drying-wetting cycles

For unsaturated concrete with initial saturations less than 1.0, the equilibrium time ratio and influential depth are also the function of the initial water saturation in the concrete. For simplicity, consider a constant initial water saturation,

$$\theta_{ini}(x) = \theta_{un}^0 < 1.0 \quad (17)$$

Stability of the wetting profiles for two consecutive cycles was defined as $\theta_k - \theta_{k-1}$ approaching a predefined numerical tolerance of 0.002, which means that the infinite norm of the vector $\theta_k - \theta_{k-1}$ satisfies

$$\|\theta_k - \theta_{k-1}\|_\infty < 0.002 \quad (18)$$

The marine splashing case used in the previous section was also used for the unsaturated case using the properties for the Concrete I in Table 1 with an initial

water saturation of 0.8 and a cycle $t_{d-w}=1$ day. Results are given for two time ratios of $\eta = 50$ and 5000 to analyze the moisture profile evolution. The profile evolutions for the two time ratios are presented in Fig. 4. Stable distributions are achieved after 5 cycles for $\eta = 5000$ and 30 cycles for $\eta = 50$.

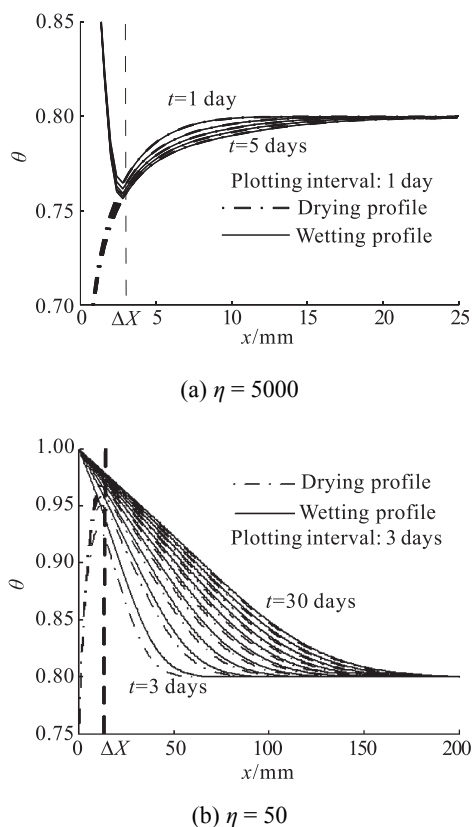


Fig. 4 Moisture profile evolution with two time ratios for unsaturated case

The results show that when η is large, the drying process dominates and the drying front passes the surface layer of material, so the influential depth near the surface is determined by the wetting process. However, if η is relatively small, the wetting process dominates and the wetting front advances into the material. Thus, the influential depth near the surface is determined by the drying period.

The results also show that there is no equilibrium time ratio for those conditions with a stable state always found for a given time ratio and that the drying and wetting periods govern the influential depth near the material surface in a more complex way. Furthermore, the number of cycles necessary to establish a stable state is relatively small compared to the actual

numbers of cycles during the service life of concrete structures, so the influential depth at the stable state can be used for durability analyses.

4 Discussion and Conclusions

The moisture influential depth into concrete was analyzed by numerically solving the differential equations. The moisture transport process was analyzed with a unified diffusion-absorption model with different diffusivities for concrete drying and wetting. The numerical results revealed several important aspects of moisture transport during drying-wetting cycles.

(1) The different moisture transport mechanisms for drying and wetting must be included in the model. The moisture transport during drying is driven by evaporation and diffusion while the moisture transport during wetting is driven by absorption. The diffusion equation can be easily solved by the finite difference method and convergence is assured by the implicit predictor-corrector scheme.

(2) The equilibrium drying-wetting time ratio was defined to balance the water loss and water absorption during each drying-wetting cycle. This equilibrium ratio can be calculated for initially saturated concrete and along with the influential depth which is linearly dependent on the square root of the drying time. A study of concrete surface exposed to daily marine splashing gave a realistic convection zone depth of $\Delta X \sim 11$ mm as the influential depth at the equilibrium time ratio.

(3) The equilibrium time can be used to predict the evolution of the influential depth for *in situ* drying-wetting cycles. For drying-wetting time ratios larger than the equilibrium one, the drying process dominates and the drying front progresses deeper into the concrete with time while the depth stabilizes for drying-wetting ratios less than the equilibrium ratio.

(4) For unsaturated initial conditions, no equilibrium ratio exists and the stable states are always reached regardless of the time ratio. For large time ratios, the drying process dominates the moisture transport in the material and the influential depth near the surface is determined by the wetting time while for smaller ratios, the wetting process dominates the moisture transport in the material and the influential depth is governed by the drying time.

(5) The model and the concept of equilibrium drying-wetting time ratio give more realistic predictions of the moisture transport in the structural concrete for use in durability analyses.

Experiments are needed to confirm the predicted influential depths of concrete structures.

References

- [1] Mehta P K. Durability-critical issues for the future. *Concrete International*, 1997, **19**(7): 27-32.
- [2] Cerny R, Rovnanikova P. Transport Processes in Concrete. London and New York: Taylor & Francis, 2002.
- [3] Wong S F, Wee T H, Swaddiwudhipong S, et al. Study of water movement in concrete. *Magazine of Concrete Research*, 2001, **53**(3): 205-220.
- [4] Meijers S J H, Bijen J M J M, De Borst R, Fraaij A L A. Computational results of a model for chloride ingress in concrete including convection, drying-wetting cycles and carbonation. *Materials and Structures*, 2005, **28**(276): 145-154.
- [5] Arfvísson J. A new algorithm to calculate the isothermal moisture penetration for periodically varying relative humidity at the boundary. *Nordic Journal of Building Physics*, 1999, **2**.
- [6] Cunningham M J. Moisture diffusion due to periodic moisture and temperature boundary conditions—An approximate steady analytical solution with non-constant diffusion coefficients. *Building and Environment*, 1992, **27**(3): 367-377.
- [7] Torrenti J M, Granger L, Diruy M, et al. Modeling concrete shrinkage under variable ambient conditions. *ACI Materials Journal*, 1999, **96**(1): 35-39.
- [8] Janssen H, Blocken B, Carmeliet J. Conservative modeling of the moisture and heat transfer in building components under atmospheric excitation. *International Journal of Heat and Mass Transfer*, 2007, **50**(5-6): 1128-1140.
- [9] Mainguy M, Coussy O, Baroghel-Bouny V. The role of air pressure in the drying of weakly permeable materials. *Journal of Engineering Mechanics ASCE*, 2001, **127**(6): 582-592.
- [10] Coussy O. Poromechanics. New York: John Wiley & Sons, 2004.
- [11] Neithalath N. Analysis of moisture transport in mortars and concrete using sorption-diffusion approach. *ACI Materials Journal*, 2006, **103**(3): 209-217.
- [12] Martys N S, Ferraris C F. Capillary transport in mortars and concrete. *Cement and Concrete Research*, 1997, **27**(5): 747-760.
- [13] Bazant Z P, Najjar L J. Nonlinear water diffusion in non-saturated concrete. *Material and Structure*, 1972, **5**(25): 3-20.
- [14] Hall C. Water sorptivity of mortars and concretes: A review. *Magazine of Concrete Research*, 1989, **41**(147): 51-61.
- [15] Leech C, Lockington D, Dux P. Unsaturated diffusivity functions for concrete derived from NMR images. *Materials and Structures*, 2003, **36**(6): 413-418.
- [16] Lockington D, Parlange J, Dux P. Sorptivity and the estimation of water penetration into unsaturated concrete. *Materials and Structures*, 1999, **32**(5): 342-347.
- [17] Lu Jinfu, Gu Lizhen, Chen Jingliang. The Difference Method for Partial Differential Equation. Beijing: Higher Education Press, 1988. (in Chinese)
- [18] Cai Dayong, Bai Fengshan. Modern Scientific Computation. Beijing: Science Press, 2000. (in Chinese)
- [19] Fédération Internationale du Béton. Model Code for Service Life Design, FIB Bulletin 34. Lausanne: FIB, 2006.